

# *p*-Difluorobenzene–Argon Ground State Intermolecular Potential Energy Surface<sup>†</sup>

José Luis Cagide Fajín and Berta Fernández\*

Department of Physical Chemistry, Faculty of Chemistry, University of Santiago de Compostela, E-15782 Santiago de Compostela, Spain

Peter M. Felker

Department of Chemistry and Biochemistry, University of California, Los Angeles, California 90095-1569

Received: July 15, 2005; In Final Form: October 4, 2005

The ground state intermolecular potential energy surface for the *p*-difluorobenzene–Ar van der Waals complex is evaluated using the coupled cluster singles and doubles including connected triple excitations [CCSD(T)] model and the augmented correlation consistent polarized valence double- $\zeta$  basis set extended with a set of 3s3p2d1f1g midbond functions. The surface minima are characterized by the Ar atom located above and below the difluorobenzene center of mass at a distance of 3.5290 Å. The corresponding binding energy is  $-398.856\text{ cm}^{-1}$ . The surface is used in the evaluation of the intermolecular level structure of the complex. The results clearly improve previously available data and show the importance of using a good correlation method and basis set when dealing with van der Waals complexes.

## I. Introduction

van der Waals complexes are well-known for playing a key role as models in the study of processes so crucial as the solvation or adsorption of molecules.<sup>1,2</sup> Series of systems constituted by an aromatic molecule to which a successive number of rare-gas atoms are added were studied as models for specific solvation steps.<sup>2</sup> van der Waals complexes constituted by aromatic molecules and rare-gas atoms have been studied intensely in the past.<sup>3</sup> In previous work we have studied the benzene–argon ground,<sup>4,5</sup> excited S<sub>1</sub>,<sup>4,6</sup> and excited T<sub>1</sub><sup>7</sup> states, evaluating highly accurate intermolecular potential energy surfaces (IPESs) using the coupled cluster singles and doubles (CCSD) model including connected triple corrections [CCSD(T)] and the aug-cc-pVDZ basis set extended with a set of 3s3p2d1f1g midbond functions (denoted 33211).<sup>4</sup> For the excited states<sup>4,6,7</sup> we used the CCSD method. In the benzene–argon ground state equilibrium configuration the Ar atom is located at  $\pm 3.5547\text{ Å}$  above and below the benzene plane on the benzene C<sub>6</sub> axis and has a dissociation energy of  $386.97\text{ cm}^{-1}$ .

Recently, we extended this work by considering the effect of a slight modification of the benzene ring, studying complexes such as the chlorobenzene–<sup>8</sup> and the fluorobenzene–argon.<sup>9</sup> In the case of the latter, we obtained a binding energy of  $391.1\text{ cm}^{-1}$  and an equilibrium geometry with the argon atom located at a distance of  $3.562\text{ Å}$  from the fluorobenzene center of mass, with an angle of  $6.33^\circ$  with respect to the axis that passes through the fluorobenzene center of mass and is perpendicular to the fluorobenzene plane. For all the studied complexes the vibrational levels obtained from the ground state IPESs agreed very well with the experimental data available and in several cases were able to correct some of the assignments. For the two excited states considered<sup>4,6,7</sup> the results were also satisfactory.

In the present study we are going to continue this work, and apply the same method and basis set to study the *p*-difluoroben-

zene–Ar complex. This complex was selected because of three main reasons: first, to provide an accurate ground state IPES, as a first step in the evaluation of the S<sub>1</sub> excited state IPESs, work that has been requested by several authors to be able to interpret their results;<sup>12</sup> second, to check the accuracy of the MP2/aug-cc-pVDZ surface of ref 13; and third, to be able to assess the effect on the IPES of a slight modification of the benzene ring by the introduction of a second fluorine atom in the para position.

The *p*-difluorobenzene–Ar has been studied from the theoretical point of view using the second-order Møller–Plesset (MP2) method. In the first of these studies, Hobza et al.<sup>10</sup> used the 6-31+G\* basis set to describe the *p*-difluorobenzene and a [7s4p2d] basis set for the argon atom. They carried out calculations for three structures given by intermolecular distances of  $3.5\text{ Å}$  ( $333\text{ cm}^{-1}$ ),  $3.6\text{ Å}$  ( $342\text{ cm}^{-1}$ ), and  $3.7\text{ Å}$  ( $336\text{ cm}^{-1}$ ). Tarakeshwar et al.<sup>11</sup> using the MP2 method and a [7s4p2d1f/4s3p1d/3s1p] basis set obtained a binding energy of  $408\text{ cm}^{-1}$  ( $D_0 = 364\text{ cm}^{-1}$ ) and a position for the argon atom on the C<sub>2</sub> axis perpendicular to the ring at a distance of  $3.578\text{ Å}$  from the *p*-difluorobenzene plane.

Recently, Moulds et al.<sup>12</sup> have studied this complex using the MP2 method and the aug-cc-pVDZ basis set. Unconstrained geometry optimization was carried out for all the stationary points. They obtained a binding energy of  $377\text{ cm}^{-1}$  and an internuclear equilibrium distance of  $3.366\text{ Å}$ . The MP2 method is found to overestimate the energy barriers, and this error is corrected by comparison with previous CCSD(T) results for the benzene–argon complex (refs 3–5). The energy barrier for the movement of the argon atom around the ring is estimated as  $\leq 204\text{ cm}^{-1}$  in the S<sub>0</sub> state and as  $\leq 225\text{ cm}^{-1}$  in the S<sub>1</sub> state. But anomalous fluorescence is observed from the  $240\text{ cm}^{-1}$  level, and the authors concluded that the evaluation of a coupled cluster S<sub>1</sub> IPES is necessary to be able to interpret the results.

The most recent theoretical study on the complex has been carried out also using the MP2 method and the aug-cc-pVDZ and aug-cc-pVDZ(-d,-2p) bases.<sup>13</sup> The latter basis set was

<sup>†</sup> Part of the special issue "Jack Simons Festschrift".

**TABLE 1: Dissociation Energies  $D_e$  and  $D_0$  in  $\text{cm}^{-1}$  and Equilibrium Distances in  $\text{\AA}$  (Comparison to Previous Results)**

	$D_0$	$R_e$	$D_e$
MP2 (ref 10)		3.6	342
MP2 (ref 11)	364	3.578	408
MP2 (ref 12)		3.366	377
MP2 (ref 13)	351.6	3.5209	402
CCSD(T)		3.5290	398.85
exp (ref 16)	$160 \leq D_0 \leq 212$	$3.5 \pm 0.5$	
exp (ref 17)		3.55	
exp (ref 19)	$337 \pm 4$		
exp (ref 36)	$339 \pm 4$		
exp (ref 20)		$3.543 \pm 0.017$	

derived from the standard aug-cc-pVDZ by removing from it some d-type functions for the heavy atoms and p-functions for the hydrogens. The geometry of the planar *p*-difluorobenzene molecule was determined by optimization of its structure with the MP2 method and the cc-pVTZ basis set. The two potential surfaces were fitted to analytic functions. These IPESs were additionally corrected using two correction functions: one taking care of the anisotropy, and the other of the region around the global minimum. These correction functions were optimized using previous CCSD(T) results.<sup>5</sup> The aug-cc-pVDZ (aug-cc-pVDZ(-d,-2p)) IPES presents a global minimum at a distance of 3.5209 (3.5264)  $\text{\AA}$  from the center of mass of the *p*-difluorobenzene molecule and a binding energy of 402 (404)  $\text{cm}^{-1}$ .

Within the experimental work carried out on the complex, Parmenter et al.<sup>14,15</sup> studied the excited state  $S_1$ , obtaining dispersed fluorescence spectra. In later work, Parmenter et al.<sup>16</sup> were able to get the fluorescence excitation spectra and identify the  $S_1 \leftarrow S_0$  absorption bands. The rotational band contours are consistent with a position of the argon atom on the axis that passes through the center of the benzene ring and is perpendicular to the *p*-difluorobenzene plane, at  $3.5 \pm 0.5$   $\text{\AA}$  from the molecular plane in the  $S_0$  state. The  $S_0$  dissociation energy  $D_0$  is estimated between 160 and 212  $\text{cm}^{-1}$ .

Neusser et al.<sup>17</sup> obtained the rovibronic spectrum of the complex and assigned the van der Waals vibronic bands up to 125  $\text{cm}^{-1}$ . In previous work<sup>18</sup> they obtained a van der Waals bond length of 3.55(2)  $\text{\AA}$  for the ground state.

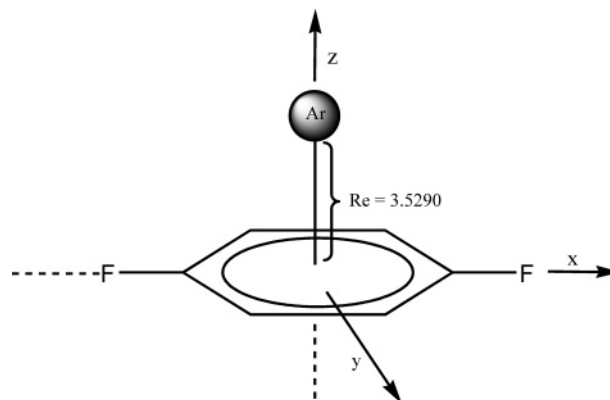
Bellm et al.<sup>19</sup> studied the *p*-difluorobenzene–Ar complex with velocity map imaging techniques and determined the dissociation energy  $D_0$  as  $337 \pm 4$   $\text{cm}^{-1}$  in the ground state. The dissociation energies determined are inconsistent with the dispersed fluorescence spectra of the complexes. They concluded that the discrepancy between their results and the dispersed fluorescence results is solved by considering transitions of the van der Waals complex shifted such that they appear at the *p*-difluorobenzene wavelengths.

Recently, Weichert et al.<sup>20</sup> have used time-resolved rotational spectroscopy to obtain the rovibrational spectrum of the complex. The equilibrium *p*-difluorobenzene–Ar distance is  $3.543 \pm 0.017$   $\text{\AA}$  in the ground state. In Table I all these results are summarized.

This paper is organized as follows: In section II we describe the computational details and analyze the IPES obtained, in section III the calculation of the intermolecular level structure, and in the last section we summarize and give our concluding remarks.

## II. Intermolecular Potential Energy Surface

To generate the *p*-difluorobenzene–Ar potential energy surface, the geometry of the *p*-difluorobenzene molecule is kept

**Figure 1.** *p*-Difluorobenzene–Ar complex intermolecular geometry ( $R_e = \pm 3.5290$   $\text{\AA}$ ).**TABLE 2: *p*-Difluorobenzene MP2/cc-pVTZ Optimized Geometry<sup>13</sup>**

length	value ( $\text{\AA}$ )	angle	value (deg)
C(H)–C(H)	1.39255	C(H)–C(H)–C(F)	118.98
C(H)–C(F)	1.3865	C(H)–C(F)–C(H)	122.03
C–F	1.3446	C(H)–C(H)–F	118.98
C–H	1.0798	C(H)–C(H)–H	121.31

fixed at that determined by Makarewicz<sup>13</sup> through a geometrical optimization using the MP2 method and the cc-pVTZ basis set. This geometry is characterized by the bond lengths and angles given in Table 2.

To cover all regions of the IPES, we evaluate the interaction energy for 439 intermolecular geometries. These geometries are described by the Cartesian coordinates ( $x, y, z$ ) of the Ar position vector  $\vec{r}$  with the origin in the *p*-difluorobenzene center of mass. The two fluorine atoms are located on the  $X$ -axis, and the  $Z$ -axis is perpendicular to the *p*-difluorobenzene plane. The molecular orientation is shown in Figure 1.

Considering the good performance we obtained in our previous studies on similar complexes, to carry out these calculations, we use the CCSD(T) method and the aug-cc-pVDZ basis set augmented with the additional set of 3s3p2d1f1g midbond functions centered in the middle of the van der Waals bond.<sup>4–6,8,9</sup> The exponents of these functions are 0.90, 0.30, and 0.10 for the s and the p functions, 0.60 and 0.20 for the d functions, and 0.30 for the g and the f functions.<sup>4</sup> We correct for the basis set superposition error with the counterpoise method of Boys and Bernardi.<sup>21</sup> The core is kept frozen in all calculations, and the interaction energies are evaluated using the DALTON<sup>22</sup> and ACESII<sup>23</sup> programs.<sup>24</sup>

The IPES of the *p*-difluorobenzene–Ar complex is constructed from the ab initio single point results by fitting them to an analytic function  $V(x, y, z)$ . Similar expansions have been previously employed with excellent results.<sup>4–9</sup>

The function  $V$  includes six terms  $V^C$ ,  $V^F$ ,  $V^H$ ,  $V^{HF}$ ,  $V^{HC}$ , and  $V^{CF}$ .  $V^C$  describes the interaction of the Ar with the carbon atoms, and it is assumed in the form

$$V^C(\vec{r}) = V_0 + W_0^C \left[ \sum_k V_2^C(r_k) + \sum_{l < k} V_3^C(r_k, r_l) + \sum_{m < l < k} V_0^C(r_k, r_l, r_m) \right] \quad (1)$$

where

$$r_k = [(x - X_k)^2 + (y - Y_k)^2 + b_z^C(z - Z_k)]^{1/2} \quad (2)$$

is a modified distance between Ar and the  $k$ th carbon atom placed at  $R_k = (X_k, Y_k, Z_k)$ .

**TABLE 3: Parameters of the Analytic IPS Fitted to the ab Initio Interaction Energies<sup>a</sup>**

	param	carbons	fluorines	hydrogens
	$r_0/\text{Å}$	4.17739	2.25565	1.68102
	$a/\text{Å}^{-1}$	0.73631	1.88101	1.89522
	$b_z/\text{Å}^{-2}$	1.00800	0.98329	0.915483
	$V_0/\text{cm}^{-1}$	-702.89		
	$W_0/\text{cm}^{-1}$	85.0921 <sup>b</sup>	492.629 <sup>c</sup>	207.934 <sup>d</sup>

param	value	term	param	value	term
C <sub>1</sub>	-17.292007	$W^3(r_k)$	C <sub>17</sub>	-8.7089471	$F(r_k) W^2(r_l)$
C <sub>2</sub>	-0.7044112	$W^4(r_k)$	C <sub>18</sub>	15.239046	$F^2(r_k) W^2(r_l)$
C <sub>3</sub>	0.2386563	$W^5(r_k)$	C <sub>19</sub>	-6.5116116	$F^3(r_k) W^2(r_l)$
C <sub>4</sub>	-18.797508	$F^3(r_k)$	C <sub>20</sub>	0.51997757	$F^2(r_k) W^3(r_l)$
C <sub>5</sub>	2.3769077	$F^4(r_k)$	C <sub>21</sub>	-43.053190	$H^6(r_k) F^{12}(r_l)$
C <sub>6</sub>	297.06584	$F^5(r_k)$	C <sub>22</sub>	-18.661351	$H^{12}(r_k) F^6(r_l)$
C <sub>7</sub>	-339.28236	$F^6(r_k)$	C <sub>23</sub>	28.469511	$H^{12}(r_k) F^{12}(r_l)$
C <sub>8</sub>	111.89507	$F^7(r_k)$	C <sub>24</sub>	29.809748	$H^6(r_k) F^6(r_l)$
C <sub>9</sub>	-23.506060	$H^3(r_k)$	C <sub>25</sub>	-0.4546509	$H^2(r_k) W^2(r_l)$
C <sub>10</sub>	8.8381665	$W(r_k) W(r_l)$	C <sub>26</sub>	0.046269685	$H^4(r_k) W^4(r_l)$
C <sub>11</sub>	-1.9418918	$W^2(r_k) W^2(r_l)$	C <sub>27</sub>	0.370955219	$H^6(r_k) W^6(r_l)$
C <sub>12</sub>	1.1620098	$W(r_k) W^2(r_l) + W^2(r_k) W(r_l)$	C <sub>28</sub>	-0.30560501	$H(r_k) W(r_l) F(r_m)$
C <sub>13</sub>	0.9211840	$W(r_k) W^3(r_l) + W^3(r_k) W(r_l)$	C <sub>29</sub>	-0.93511871	$W(r_k) W(r_l) W(r_m)$
C <sub>14</sub>	-0.0195374	$W^3(r_k) W^2(r_l) + W^2(r_k) W^3(r_l)$	C <sub>30</sub>	-0.7979169	$F(r_k) W(r_l) W(r_m)$
C <sub>15</sub>	3.6895771	$F(r_k) W(r_l)$	C <sub>31</sub>	0.040272251	$F^2(r_k) W^2(r_l) W^2(r_m)$
C <sub>16</sub>	-2.3763267	$F^2(r_k) W(r_l)$			

<sup>a</sup>  $W(r_k)$  refers to the carbon,  $F(r_k)$  to the fluorine, and  $H(r_k)$  to the hydrogen atoms. <sup>b</sup> Used for terms including only  $W^i(r_k)$ . <sup>c</sup> Used for terms including  $F^i(r_k)$  but not  $H^i(r_k)$ . <sup>d</sup> Used for all terms including  $H^i(r_k)$ .

**TABLE 4: Basis Set and Grid Parameters for Calculation of *p*-Difluorobenzene (pDFB)–Ar  $J = 0$  States**

$\gamma_x = 2.699587 \text{ Å}^{-1}$	$\gamma_y = \gamma_x$	$\gamma_z = 8.098761 \text{ Å}^{-1}$
$x_0 = y_0 = 0$	$z_0 = 3.5 \text{ Å}$	$N_x = N_y = N_z = 40$
$I_x = 89.6445 \text{ amu Å}^2$	$I_y = 353.908 \text{ amu Å}^2$	$I_z = 443.549 \text{ amu Å}^2$
$m_{\text{pDFB}} = 114.0312 \text{ amu}$	$m_{\text{Ar}} = 39.948 \text{ amu}$	$\mu = 29.5849 \text{ amu}$

The two-body potential term is represented by a Morse type expansion

$$V_2(r_k) = w^2(r_k) + \sum_{i=3}^8 c_i w^i(r_k) \quad (3)$$

where

$$w(r_k) = 1 - \exp(-a(r_k - r_0)) \quad (4)$$

The three-(four-)body potential term  $V_3^C(V_0^C)$  is the sum of the different 3-(4-)body terms given in Table 4 for the carbons (they are denoted as  $W^i(r_k)$ ).

The  $V^F$  and  $V^H$  potentials represent the two-body interaction of the Ar atom with the fluorine and hydrogen atoms, respectively, and are defined by Morse-type functions analogous to that given in eq 3.

The mixed terms  $V^{\text{CF}}$ ,  $V^{\text{HF}}$ , and  $V^{\text{HC}}$  represent the three- and four-body interactions among the Ar, the carbons, the fluorine, and the hydrogen atoms. The explicit forms of the properly selected three- and four-body terms for the  $V^{\text{CF}}$ ,  $V^{\text{HF}}$ , and  $V^{\text{HC}}$  are collected in Table 3 (they are referred as  $W^i(r_k)$  for the carbons,  $F^i(r_k)$  for the fluorine, and  $H^i(r_k)$  for the hydrogens). The fitted values of the IPES parameters are also given in Table 3.

The determined IPES reproduces all the ab initio values with a standard error of 0.02. The maximum residual is of 1.9216  $\text{cm}^{-1}$ , at the intermolecular geometry given by  $(x, y, z) = (-3.4470, 0.0000, 2.8925) \text{ Å}$  and with an energy of  $-57.733 \text{ cm}^{-1}$ .

The absolute minima of the interaction energy between the Ar atom and the *p*-difluorobenzene molecule are located above

and below the center of mass of the *p*-difluorobenzene in two equivalent positions at distances of  $\pm 3.5290 \text{ Å}$  from the center of the ring and with binding energies of  $-398.856 \text{ cm}^{-1}$ . The complex equilibrium geometry is shown in Figure 1. Comparing these results to those previously available (see Table 1), we can see that the dissociation energy  $D_e$  is very close to that determined in ref 13, and therefore, we can expect a similar value for  $D_0$  as that obtained in this reference. This result is quite far from the experimental limits  $160 \leq D_0 \leq 212 \text{ cm}^{-1}$  of ref 16, but close to the most recent result of  $339 \pm 4 \text{ cm}^{-1}$ .<sup>36</sup> Regarding the bond distance, our result clearly improves those previously available, and it is within the error limits of the most accurate experimental distance ( $3.543 \pm 0.017 \text{ Å}$ ).<sup>20</sup>

For further testing the accuracy of the previous MP2–IPESs,<sup>13</sup> we compare these surfaces to ours in the different regions. In Figure 2a–d we show the contour plots for the CCSD(T) and the MP2 aug-cc-pVDZ IPES of ref 13 in the  $y = 0$ ,  $x = 0$ ,  $z = Z_c$ , and  $z = 0$  planes. The IPESs are quite similar in the areas around the absolute minima, with differences of  $\sim 3 \text{ cm}^{-1}$  (5  $\text{cm}^{-1}$  when comparing to the MP2 aug-cc-pVDZ(-d,-2p) basis set IPES), but in the other regions the differences are significant, going up to 98.9  $\text{cm}^{-1}$  (143.2  $\text{cm}^{-1}$  when comparing to the MP2 aug-cc-pVDZ(-d,-2p) basis set IPES). The largest differences correspond to the  $(x, y, z) = (0.0, 4.5, 0.0) \text{ Å}$  geometry.

When comparing the *p*-difluorobenzene–Ar IPES with those obtained for the benzene–Ar and the fluorobenzene–Ar complexes using the same method and basis set, we see that the addition of a second fluorine atom gives rise to a much stronger interaction (the fluorobenzene–Ar and the benzene–Ar IPESs are very similar).<sup>9</sup> In this way, the dissociation energy of the complex increases considerably by the addition of a second F atom to the ring (7.8  $\text{cm}^{-1}$  compared to 4.1  $\text{cm}^{-1}$  due to the addition of the first F atom) and, correspondingly, the equilibrium distance gets shorter (0.033 Å shorter compared to the fluorobenzene–Ar complex).

### III. Calculation of the Intermolecular Level Structure

**A. Vibrational ( $J = 0$ ) States.** The intermolecular level structure corresponding to the fitted IPES was computed

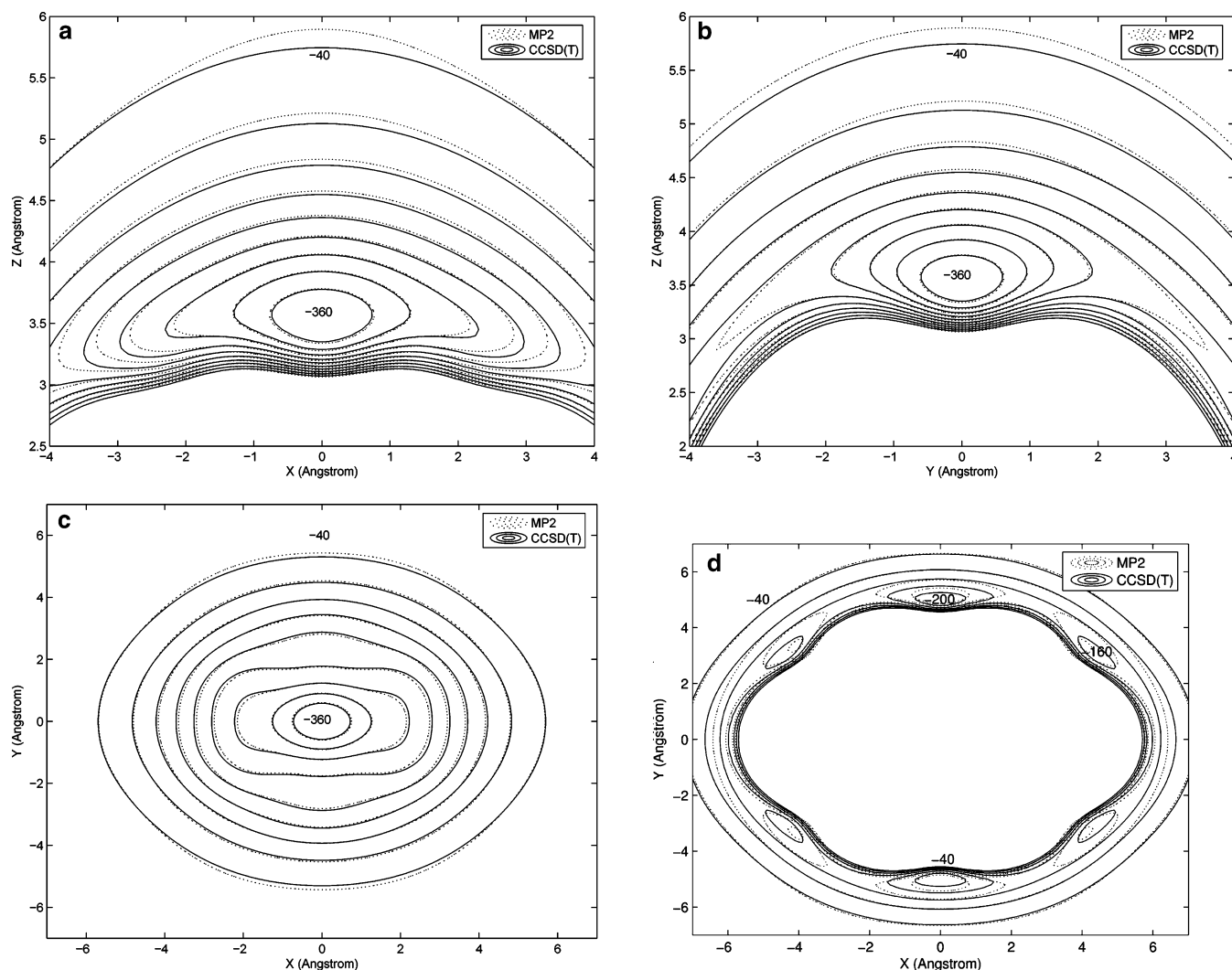


**Figure 2.** Contour plots of the CCSD(T) IPES of the present work and the MP2 IPES of ref 13: in the  $y = 0$  plane (a), in the  $x = 0$  plane (b), in the  $xy$  plane at  $z = z_c$  (c), and at  $z = 0$  (d). The values of subsequent contours differ by  $40 \text{ cm}^{-1}$ .

variationally by using filter diagonalization<sup>25,26</sup> to diagonalize the  $J = 0$  Hamiltonian<sup>27,28</sup> (in atomic units)

$$\hat{H}_v = \hat{T}_v + V(x,y,z) = -\frac{\nabla^2}{2\mu} + \sum_k \frac{\hat{l}_k^2}{2I_k} + V(x,y,z) \quad (5)$$

Here,  $x$ ,  $y$ , and  $z$  are identical to the coordinates defined in section II,  $\nabla^2$  is the Laplacian expressed in these coordinates,  $\hat{l}_k$  is the operator corresponding to the component of the orbital angular momentum of the complex as measured along the  $k = \hat{x}$ ,  $\hat{y}$ , or  $\hat{z}$  body-fixed axis,  $I_k$  is the moment of inertia of *p*-difluorobenzene about that moiety's principal axis parallel to  $k$ ,  $\mu$  is the reduced mass of the complex, and  $V(x,y,z)$  is the fitted IPES. The particular values used here for the molecular parameters appearing in  $\hat{H}_v$  are given in Table 4.

Filter diagonalization, as applied here, requires repeated application of  $\hat{H}_v$  to an initial, random state vector  $|\Psi_0\rangle$ . State vectors were expressed in a discrete variable representation (DVR) basis composed of triple products of one-dimensional DVRs<sup>28</sup>

$$|a,b,c\rangle \equiv |x_a\rangle|y_b\rangle|z_c\rangle \quad (6)$$

The one-dimensional DVRs are defined in terms of one-dimensional harmonic oscillator eigenfunctions ( $\varphi_n$ ) and the

Gauss–Hermite quadrature points and weights associated with those functions. Thus, the  $N_x$  functions of the  $x$ -dependent DVR are given by

$$|x_a\rangle \equiv \sum_{n=0}^{N_x-1} \sqrt{w_n} \phi_n(x_a) \phi_n(\gamma_x[x-x_0]) \quad (7)$$

where  $x_a$  is a quadrature point,  $w_n$  is its associated weight, and  $\gamma_x$  and  $x_0$  are chosen to tailor the DVR to the IPES. Analogous expressions apply to the  $N_y|y_b\rangle$  and the  $N_z|z_c\rangle$  DVRs. The specific values of all the DVR parameters chosen for this work are given in Table 5. The full primitive basis has dimension  $N_x \times N_y \times N_z = 64\,000$ .

Application of  $\hat{H}_v$  to a given state vector  $|\Psi\rangle$  was accomplished in two steps. First, matrix elements of  $\hat{T}_v$  in the harmonic-oscillator basis isomorphic to the  $|a,b,c\rangle$  basis were computed analytically and then transformed to the DVR basis by using eq 7 and its analogues for the other two dimensions.  $\hat{T}_v|\Psi\rangle$  was then obtained by matrix-vector multiplication. Second,  $V|\Psi\rangle$  was computed by making use of the fact that the matrix of  $V$  in the DVR basis is diagonal, with nonzero elements given by  $\langle a,b,c|V|a,b,c\rangle = V(x_a,y_b,z_c)$ . Thus, operation with  $V$  on  $|\Psi\rangle$  was straightforward.

Filter diagonalization was applied by computing from  $|\Psi_0\rangle$  “window-basis” functions at selected energies within a set

**TABLE 5: Properties of Calculated  $J = 0$  States for  $p$ -Difluorobenzene–Ar**

$N$	$\Gamma$	$\Delta E^a$	$\langle z \rangle^b$	$\langle \Delta z \rangle^b$	$\langle \Delta x \rangle^b$	$\langle \Delta y \rangle^b$	$n_x, n_y, n_z$
0	A <sub>1</sub>	0.0	3.575	0.116	0.255	0.293	0,0,0
1	B <sub>1</sub>	18.1	3.585	0.117	0.459	0.301	1,0,0
2	A <sub>1</sub>	33.4	3.598	0.131	0.598	0.316	2,0,0
3	B <sub>2</sub>	34.3	3.595	0.119	0.270	0.532	0,1,0
4	A <sub>1</sub>	41.6	3.631	0.191	0.321	0.352	0,0,1
5	B <sub>1</sub>	47.3	3.605	0.133	0.758	0.328	3,0,0
6	A <sub>2</sub>	50.7	3.605	0.120	0.489	0.549	1,1,0
7	A <sub>1</sub>	59.5	3.609	0.134	0.921	0.344	4,0,0
8	B <sub>1</sub>	59.9	3.642	0.191	0.531	0.369	1,0,1
9	B <sub>2</sub>	64.2	3.616	0.133	0.641	0.579	2,1,0
10	A <sub>1</sub>	66.8	3.619	0.132	0.297	0.708	0,2,0
11	B <sub>1</sub>	70.1	3.606	0.135	1.099	0.363	5,0,0
12	B <sub>2</sub>	71.8	3.647	0.184	0.348	0.642	0,1,1
13	A <sub>1</sub>	73.5	3.658	0.212	0.686	0.392	2,0,1
14	A <sub>2</sub>	76.2	3.619	0.133	0.828	0.603	3,1,0
15	A <sub>1</sub>	79.1	3.612	0.167	1.198	0.391	6,0,0
16	A <sub>1</sub>	81.2	3.674	0.229	0.604	0.422	0,0,2
17	B <sub>1</sub>	81.5	3.627	0.136	0.561	0.724	1,2,0
18	B <sub>1</sub>	84.9	3.612	0.178	1.268	0.409	7,0,0
19	B <sub>2</sub>	86.4	3.616	0.135	1.031	0.634	4,1,0
20	A <sub>2</sub>	88.0	3.654	0.184	0.593	0.674	1,1,1
21	B <sub>1</sub>	88.8	3.630	0.192	1.146	0.426	3,0,1
22	A <sub>1</sub>	92.0	3.582	0.160	1.470	0.519	8,0,0
23	A <sub>1</sub>	93.5	3.620	0.151	0.970	0.715	2,2,0
24	A <sub>2</sub>	94.8	3.601	0.138	1.269	0.675	5,1,0
25	B <sub>2</sub>	96.8	3.646	0.160	0.475	0.873	0,3,0
26	B <sub>1</sub>	98.8	3.619	0.211	1.312	0.490	1,0,2
27	B <sub>2</sub>	99.7	3.619	0.179	1.144	0.722	2,1,1
28	A <sub>1</sub>	100.0	3.664	0.187	0.403	0.863	0,2,1

<sup>a</sup> Energy in cm<sup>-1</sup> relative to the zero-point energy at -348.57 cm<sup>-1</sup>.

<sup>b</sup> Quoted values are in Å.

energy window. These functions were accumulated for 1024 applications of  $\hat{H}_v$  by using the Chebyshev method embodied in eq 6 of ref 26. For the final results quoted below, filtering at 50 energies between -353.4 and -219.5 cm<sup>-1</sup> was used. Many of these energies were obtained as eigenvalues from a prior filter-diagonalization run employing fewer Chebyshev steps. The remaining were chosen at equally spaced intervals within the above range.

The window-basis functions computed as above could immediately have been employed as a basis in which to diagonalize  $\hat{H}_v$  and obtain eigenfunctions and eigenvalues for the chosen energy window. Instead of doing this, though, we first made use of the symmetry of  $p$ -difluorobenzene–Ar to obtain symmetry-factored results. For  $p$ -difluorobenzene–Ar, in which tunneling of Ar from one side of the aromatic plane to the other is taken to be not feasible, the molecular symmetry group is  $G_4$  (isomorphic with point group  $C_{2v}$ ).<sup>13</sup> Each of the window functions was symmetrized<sup>29</sup> so as to transform as one of the irreducible representations of the  $G_4$  molecular symmetry group. This was done by applying the projection operator  $\hat{P}_{\epsilon,\delta}$  to the window basis.

$$\hat{P}_{\epsilon,\delta} = \sum_{a,b,c} |a,b,c,\epsilon,\delta\rangle \langle a,b,c,\epsilon,\delta| \quad (8)$$

where the

$$|a,b,c,\epsilon,\delta\rangle \equiv [|a,b,c\rangle + (-1)^\epsilon |-a,b,c\rangle + (-1)^\delta |a,-b,c\rangle + (-1)^{\epsilon+\delta} |-a,-b,c\rangle] \quad (9)$$

are symmetry-adapted basis functions, the values of  $\epsilon$  and  $\delta$  determine the  $G_4$  irrep to which  $\hat{P}_{\epsilon,\delta}$  corresponds (0,0 = A<sub>1</sub>, 1,1 = A<sub>2</sub>, 1,0 = B<sub>1</sub> and 0,1 = B<sub>2</sub>), and the range of the summation included in eq 8 encompasses all the  $z_c$  DVRs but

only the DVRs corresponding to positive  $x_a$  and  $y_b$ . Once symmetry-filtered, the window basis for a particular irrep was re-expressed in the eq 6 basis. The functions were orthogonalized by the Gram–Schmitt procedure. The matrix of  $\hat{H}_v$  in the resulting basis was computed and, finally, diagonalized numerically.

Table 5 presents results of the  $J = 0$  calculations for all states computed to be less than 100 cm<sup>-1</sup> above the zero point, which is at -348.57 cm<sup>-1</sup>. The assignments of the states given in the table are based on (a) the values of the root-mean-squared deviations in  $x$ ,  $y$ , and  $z$  ( $\langle \Delta x \rangle$ ,  $\langle \Delta y \rangle$ , and  $\langle \Delta z \rangle$ ) for each eigenfunction and (b) the nodal structure of that eigenfunction. The assignments are given in terms of the numbers of quanta in each of the three intermolecular modes, denoted as  $n_x$ ,  $n_y$ , and  $n_z$ , in conformity with the nomenclature of ref 13. These three modes correspond, respectively, to relative translational motion of the Ar and  $p$ -difluorobenzene in the  $\hat{x}$ ,  $\hat{y}$ , and  $\hat{z}$  directions.

Comparison of the results of Table 5 with the results of the intermolecular level-structure calculations of ref 13, based on the MP2-derived IPES, reveals substantial agreement. The present results yield a  $D_0$  value several cm<sup>-1</sup> closer to experimental values (see Table 1). The fundamental frequencies of the intermolecular stretching mode (41.6 cm<sup>-1</sup> here vs 41.7 cm<sup>-1</sup> in ref 13) and the bending mode along the  $\hat{y}$  axis (34.3 cm<sup>-1</sup> for both) are close to each other and to experimental values (though the experimental results pertain to the S<sub>1</sub> electronic state, not S<sub>0</sub>).<sup>17</sup> The most significant discrepancy between the two sets of calculated results derives from the difference in the fundamental frequency of the  $\hat{x}$  bending mode (18.1 cm<sup>-1</sup> here vs 17.7 cm<sup>-1</sup> in ref 13). This gives rise to increasing differences in the calculated level structures as the energy increases. Clearly, experimental information on the S<sub>0</sub> intermolecular states of  $p$ -difluorobenzene–Ar would be valuable in further assessing the accuracy of the computed IPESs.

**B. Rotational Level Structures.** The rotational energy levels corresponding to a given intermolecular vibrational state were calculated by the “Eckart method” described in ref 30. This method makes the approximation that in a properly chosen body-fixed Eckart frame (BF<sub>E</sub>) the rotational and vibrational degrees of freedom are separable. With this assumption the rotational states of a given vibrational state can be computed if the  $J = 0$  vibrational eigenstate in an arbitrary body-fixed axis system (BF<sub>A</sub>) is known and if one knows how to transform between BF<sub>A</sub> and BF<sub>E</sub>. The computed states are accurate to the extent that rotational–vibrational coupling is eliminated in BF<sub>E</sub>.

Rovibrational eigenstates corresponding to vibrational eigenstate  $\varphi_i$  and total rotational angular momentum quantum number  $J$  are obtained by diagonalizing the  $(2J + 1) \times (2J + 1)$  Hamiltonian matrix whose elements are given by

$${}_E \langle \phi_i; JK | \hat{H} | \phi_i; JK \rangle_E \quad (10)$$

where  $|\phi_i; JK\rangle_E$  is the product of the  $i$ th vibrational eigenfunction  $\varphi_i$  and the symmetric-top eigenfunction  $|JK\rangle$  (with  $M$  quantum number suppressed, because results are independent of it), both expressed in terms of BF<sub>E</sub> coordinates, and  $\hat{H}$  is the rotational–vibrational Hamiltonian in the BF<sub>E</sub> frame. These matrix elements are evaluated by re-expressing them in terms of BF<sub>A</sub> coordinates, yielding<sup>30</sup>

$${}_E \langle \phi_i; JK | \hat{H} | \phi_i; JK \rangle_E = \sum_{k,k'} {}_A \langle D_{k,k'}^{(J)} \phi_i; Jk | \hat{H}_v + \hat{H}_{\text{rv}} | D_{k',k'}^{(J)*} \phi_i; Jk' \rangle_A \quad (11)$$

**TABLE 6: Calculated Rotational Constants (cm<sup>-1</sup>) for Selected Intermolecular Vibrational States of *p*-Difluorobenzene–Ar**

vibrational state	A	B	C
(0,0,0)	0.03819	0.03590	0.02293
	(0.03801) <sup>a</sup>	(0.03645) <sup>a</sup>	(0.02320) <sup>a</sup>
(1,0,0)	0.03849	0.03565	0.02275
(2,0,0)	0.03878	0.03538	0.02257
(0,1,0)	0.03830	0.03516	0.02261
(0,2,0)	0.03844	0.03436	0.02227
(0,0,1)	0.03828	0.03504	0.02253
(0,0,2)	0.03883	0.03423	0.02206

<sup>a</sup> Experimental values taken from ref 18.

where  $|\phi_i; Jk\rangle_A$  is the product of the  $i$ th  $J = 0$  eigenfunction and symmetric top rotational eigenfunction expressed in terms of BF<sub>A</sub> coordinates, the  $D_{k,k}^{(J)}$  are Wigner matrix elements that depend on the Euler angles,  $\omega$ , that rotate BF<sub>A</sub> into BF<sub>E</sub>,  $\hat{H}_v$  is given by eq 5, and

$$\hat{H}_{rv} = \sum_k \frac{\hat{J}_k^2 - 2\hat{J}_k \hat{l}_k}{2I_k} \quad (12)$$

where  $\hat{J}_k$  is the operator corresponding to the component of the total angular momentum of the complex measured with respect to the  $k$ th axis of BF<sub>A</sub> and  $\hat{l}_k$  and  $I_k$  are defined as above. The rhs of eq 11 can be straightforwardly evaluated for *p*-difluorobenzene–Ar from the  $\phi_i$  results of the preceding subsection by using an algorithm that computes the  $\omega$  Euler angles for each of the quadrature points corresponding to the DVR basis functions.

Rotational energies were computed as  $E - E_i$ , with rovibrational energy  $E$  obtained from the diagonalization of the matrix defined by eq 10 for a given  $J$  and  $E_i$  the vibrational eigenvalue corresponding to  $\phi_i$ . In all cases, asymmetric-top energy-level patterns were found to characterize the *p*-difluorobenzene–Ar species. As such, three rotational constants for a given  $\phi_i$  could be calculated by making use of the relations between those constants and the three  $J = 1$  rotational eigenvalues.<sup>31</sup> Table 6 presents the results of computed rotational constants for several selected intermolecular states of *p*-difluorobenzene–Ar. Also included in Table 6 are rotational constants obtained from experiment<sup>17,18</sup> for the zero-point of S<sub>0</sub>. Clearly, the agreement between experiment and calculation is quite good, with deviations only on the order of 1%. Moreover, it is important to point out that the experimental values were extracted from the data by using two approximations.<sup>18</sup> First,  $A$  for the complex was fixed to the value of  $C$  for the zero-point level of bare *p*-difluorobenzene. Second, to obtain  $B$  and  $C$ , the complex was taken to be rigid (no vibrational averaging) with the Ar atom on the  $\hat{z}$  axis. Although these approximations are not unreasonable, they could readily account for some of the small discrepancies between the experimental and calculated rotational constants.

**C. Selected Vibronic-Band Intensities.** A persistent problem in the spectroscopy of weakly bound complexes relates to the explication of the relative intensities of dipole-induced vibronic transitions that involve a change in intermolecular vibrational state during the course of an electronic transition. For such transitions in which the symmetry of the intermolecular vibrational state is the same in ground and excited electronic states, the predominant factor in determining intensity is often just a Franck–Condon factor (e.g., see ref 13). The intensity of a band of this type can often, therefore, be attributed semiquantitatively to known shifts in equilibrium geometry and/

or vibrational frequency in going from the ground to excited electronic state. In the case of *p*-difluorobenzene–Ar S<sub>1</sub> ← S<sub>0</sub> bands corresponding to the fundamental and first overtone of the intermolecular stretching vibration (that is, (0,0,1) ← (0,0,0) and (0,0,2) ← (0,0,0)), observed at 0<sub>0</sub><sup>0</sup> + 41.549 cm<sup>-1</sup> and 0<sub>0</sub><sup>0</sup> + 80.652 cm<sup>-1</sup>, respectively, are of this type.<sup>17</sup>

When there is a change in vibrational symmetry during the course of the vibronic transition, however, the Franck–Condon factor is identically zero and a calculation of relative intensity must account explicitly for the dependence of the electronic transition dipole moment on the intermolecular coordinates. Some groups suggest addressing this by employing a Herzberg–Teller approach to expand electronic wave functions in Taylor series about equilibrium nuclear positions (e.g., see ref 32). Others have used quantum chemical methods to calculate directly electronic wave functions on a grid of nuclear configurations (e.g., ref 13). The main challenge with both approaches is that they require accurate wave functions of excited electronic states, which can be difficult to obtain for species such as *p*-difluorobenzene–Ar. An alternative approach<sup>33,34</sup> is one that makes use of the fact that the S<sub>1</sub> ← S<sub>0</sub> transition in a complex like *p*-difluorobenzene–Ar is essentially a *p*-difluorobenzene-localized transition. It is a reasonable approximation, therefore, to take the electronic transition dipole to be the same as in the bare molecule, that is, pointing along the  $\hat{y}$  axis of *p*-difluorobenzene. The transition moment for a vibronic transition in a species such as *p*-difluorobenzene–Ar can then be obtained by computing the vibrational matrix element of the bare-molecule-localized transition dipole in the Eckart frame of the complex. A prescription for doing this has been presented in eq 5.3 of ref 34 and has been applied with success to benzene–Ar. Such a calculation requires only knowledge of the electronic transition dipole matrix element in the bare molecule, the intermolecular vibrational wave functions involved in the vibronic transition, and the Euler angles that rotate a frame fixed in the bare molecule into BF<sub>E</sub> of the complex.

We have calculated intensities for several S<sub>1</sub> ← S<sub>0</sub> intermolecular bands of interest in *p*-difluorobenzene–Ar. For the (0,1,0) ← (0,0,0) vibronic band we used the method described in the preceding paragraph. The results of section III.A were used for the relevant ground and excited state intermolecular eigenfunctions. For the (0,0,1) ← (0,0,0) and (0,0,2) ← (0,0,0) bands Franck–Condon factors were calculated by modeling the van der Waals stretching mode in both electronic states as a one-dimensional Morse oscillator<sup>35</sup> with parameters chosen to match the experimental results. That is, for the Morse potential in both electronic states the same fundamental frequency (41.5 cm<sup>-1</sup>) applied, but the equilibrium Ar position was set equal to  $z''_e = 3.529$  Å in the ground state and  $z'_e = 3.469$  Å in the excited state.

Similar to the results of ref 13, our results predict an appreciable intensity for the stretching fundamental (6.5% of the 0<sub>0</sub><sup>0</sup> band of the complex) and one a couple orders of magnitude less (0.02%) for the stretching overtone. The important new result, however, is the prediction of appreciable relative intensity (0.43%) for the (0,1,0) ← (0,0,0) band. Indeed, our value is 2 orders of magnitude larger than that obtained in ref 13. The result is significant because experiment shows the band in question to be one of the three strongest van der Waals features in the *p*-difluorobenzene–Ar vibronic spectrum. The present work shows that this intensity is readily understandable in terms of the vibrational averaging of the *p*-difluorobenzene-localized transition moment. One expects that the determination of an accurate IPES for the S<sub>1</sub> state of the species, similar to

that produced for benzene–Ar<sup>4,6,7</sup> will go a long way toward understanding the intensities of all the observed van der Waals vibronic bands.

#### IV. Summary and Conclusions

The CCSD(T) model together with the aug-cc-pVDZ-33211 basis set is an excellent combination to determine accurate IPESs for “large” van der Waals complexes. An extensive number of interaction energies are evaluated for the *p*-difluorobenzene–Ar complex using this method and basis set. After the interaction energies are fit to an analytical function, the obtained IPES is characterized by two equivalent minima with the argon atom located below and above the *p*-difluorobenzene center of mass, at a distance of  $\pm 3.5290$  Å and with a binding energy of  $-398.856$  cm<sup>-1</sup>.

This IPES is clearly better than the previously available MP2 surfaces and has been compared in detail to those in ref 13. With respect to the aug-cc-pVDZ MP2 IPES, near the absolute minima the differences in the energies are on the order of 3 cm<sup>-1</sup>, but in other regions they reach values up to 98.9 cm<sup>-1</sup>.

When comparing the benzene– and fluorobenzene–Ar IPESs, we see that the addition of a second fluorine atom makes the interaction between the Ar atom and the aromatic molecule considerably stronger, the changes in the IPES shape with respect to the fluorobenzene–Ar IPES being much larger than those observed when the benzene–Ar is compared to the fluorobenzene–Ar IPES.

The intermolecular level structure has been evaluated from the IPES, and good agreement is obtained with respect to the experimental results available. Regarding the results in ref 13, the major difference is the prediction of an appreciable intensity for the (0,1,0) ← (0,0,0) band.

This work is also a first step for the evaluation of the S<sub>1</sub> excited state IPES.

**Acknowledgment.** We thank Prof. Jan Makarewicz for providing the MP2 IPES. This work has been supported by the European Research and Training Network NANOQUANT, contract No. MRTN-CT-2003-506842, and by the Spanish Comisión Interministerial de Ciencia y Tecnología and FEDER (BQU2002-02484 project). We acknowledge CPU time from CESGA.

#### References and Notes

- (1) Leutwyler, S.; Bösigler, J. *Chem. Rev.* **1990**, *90*, 489.
- (2) Weber, Th.; Neusser, H. J. *J. Chem. Phys.* **1991**, *94*, 7689.
- (3) Kukolich, S. G.; Shea, J. A. *J. Chem. Phys.* **1982**, *77*, 5242. Hobza, P.; Selzle, H. L.; Schlag, E. W. *Chem. Rev.* **1994**, *94*, 1767. Felker, P. M.; Maxton, P. M.; Schaeffer, M. W. *Chem. Rev.* **1994**, *94*, 1787. Klopper, W.; Lüthi, H. P.; Brubacher, Th.; Bauder, A. *J. Chem. Phys.* **1994**, *101*, 9747. Sussmann, R.; Neuhauser, R.; Neusser, H. J. *J. Chem. Phys.* **1995**, *103*, 3315.
- (4) Koch, H.; Fernández, B.; Christiansen, O. *J. Chem. Phys.* **1998**, *108*, 2784.
- (5) Koch, H.; Fernández, B. *J. Chem. Phys.* **1999**, *111*, 198.
- (6) Fernández, B.; Koch, H.; Makarewicz, J. *J. Chem. Phys.* **1999**, *111*, 5922.
- (7) López Cacheiro, J.; Fernández, B.; Koch, H.; Makarewicz, J.; Hold, K.; Jørgensen, P. *J. Chem. Phys.* **2003**, *119*, 4762.
- (8) Munteanu, C. R.; López Cacheiro, J.; Fernández, B.; Makarewicz, J. *J. Chem. Phys.* **2004**, *121*, 1390.
- (9) Cagín Fajide, J. L.; López Cacheiro, J.; Fernández, B.; Makarewicz, J. *J. Chem. Phys.* **2004**, *120*, 8582.
- (10) Hobza, P.; Selzle, H. L.; Schlag, E. W. *J. Chem. Phys.* **1993**, *99*, 2809.
- (11) Tarakeshwar, P.; Kim, K. S.; Kraka, E.; Cremer, D. *J. Chem. Phys.* **2001**, *115*, 6018.
- (12) Moulds, R. J.; Buntine, M. A.; Lawrance, W. D. *J. Chem. Phys.* **2004**, *121*, 4635.
- (13) Makarewicz, J. *J. Chem. Phys.* **2005**, *122*, 114312.
- (14) Butz, K. W.; Catlett, D. L.; Ewing, G. E.; Krajnovich, D.; Parmenter, C. S. *J. Phys. Chem.* **1986**, *90*, 3533.
- (15) O, H.-K.; Parmenter, C. S.; Su, M. C. *Ber. Bunsen-Ges. Phys. Chem.* **1988**, *92*, 253.
- (16) Su, M. C.; O, H.-K.; Parmenter, C. S. *Chem. Phys.* **1991**, *156*, 261.
- (17) Sussmann R.; Neusser, H. J. *J. Chem. Phys.* **1995**, *102*, 3055.
- (18) Sussmann, R.; Neuhauser, R.; Neusser, H. J. *Can. J. Phys.* **1994**, *72*, 1179.
- (19) Bellm, S. M.; Moulds, R. J.; Lawrance, W. D. *J. Chem. Phys.* **2001**, *115*, 10709.
- (20) Weichert, A.; Riehn, C.; Matylytsky, V. V.; Jarzaba, W.; Brutschy, B. *J. Mol. Struct.* **2002**, *612*, 325.
- (21) Boys, S. F.; Bernardi, F. *Mol. Phys.* **1970**, *19*, 553.
- (22) Helgaker, T.; Jensen, H. J. Aa.; Jørgensen, P.; Olsen, J.; Ågren, H.; Andersen, T.; Bak, K. L.; Bakken, V.; Christiansen, O.; Dahle, P.; Dalskov, E. K.; Enevoldsen, T.; Fernández, B.; Heiberg, H.; Hetttema, H.; Jonsson, D.; Kirpekar, S.; Kobayashi, R.; Koch, H.; Mikkelsen, K. V.; Norman, P.; Packer, M. J.; Ruud, D.; Saue, T.; Taylor, P. R.; Vahtras, O. *DALTON beta-0.97*, an electronic structure program; 1997.
- (23) Stanton, J. F.; Gauss, J.; Watts, J. D.; Nooijen, M.; Oliphant, N.; Perera, S. A.; Szalay, P. G.; Lauderdale, W. J.; Kucharski, S. A.; Gwaltney, S. R.; Beck, S.; Balkova, A.; Bernholdt, D. E.; Baeck, K. K.; Rozyczko, P.; Sekino, H.; Hober, C.; Bartlett, R. J.; Almlöf, J.; Taylor, P. R.; Helgaker, T.; Jensen, H. J. Aa.; Jørgensen, P.; Olsen, J.; Taylor, P. R. *ACES II is a program product of the Quantum Theory Project*; University of Florida, 1996.
- (24) The interaction energy results can be obtained from the authors on request.
- (25) Neuhauser, D. *J. Chem. Phys.* **1990**, *93*, 2611. Neuhauser, D. *J. Chem. Phys.* **1994**, *100*, 5076. Wall, M. R.; Neuhauser, D. *J. Chem. Phys.* **1995**, *102*, 8011.
- (26) Mandelshtam, V. A.; Taylor, H. S. *J. Chem. Phys.* **1997**, *106*, 5085.
- (27) van der Avoird, A. *J. Chem. Phys.* **1993**, *98*, 5327.
- (28) For example, see Mandziuk, M.; Bačić, Z. *J. Chem. Phys.* **1993**, *98*, 7165.
- (29) For example, see Felker, P. M.; Neuhauser, D. *J. Chem. Phys.* **2003**, *119*, 5558.
- (30) Felker, P. M. *J. Chem. Phys.* **2001**, *114*, 7901.
- (31) Levine, I. N. *Molecular Spectroscopy*; Wiley: New York, 1975; p 216.
- (32) Sussmann, R.; Neuhauser, R.; Neusser, H. J. *Chem. Phys. Lett.* **1994**, *229*, 13.
- (33) Maxton, P. M.; Schaeffer, M. W.; Ohline, S. M.; Kim, W.; Ventura, V. A.; Felker, P. M. *J. Chem. Phys.* **1994**, *101*, 8391.
- (34) Felker, P. M.; Neuhauser, D.; Kim, W. *J. Chem. Phys.* **2001**, *114*, 1233.
- (35) See ref 32, p 161. The three-parameter Morse function employed for is fixed by the vibrational frequency, the equilibrium distance, and the dissociation energy. The values used for the former two parameters are quoted in the text. For  $D_e$ , 398.85 cm<sup>-1</sup> was used.
- (36) Bellm, S. M.; Gascooke, J. R.; Lawrance, W. D. *Chem. Phys. Lett.* **2000**, *330*, 103.